Letter

Quantum-correlated photons generated by nonlocal electron transport

Felicitas Hellbach [1], Fabian Pauly [2], Wolfgang Belzig [1], and Gianluca Rastelli [1,3]
[1] *Fachbereich Physik, Universität Konstanz, 78457 Konstanz, Germany*
[2] *Institute of Physics, University of Augsburg, 86135 Augsburg, Germany*
[3] *INO-CNR BEC Center and Dipartimento di Fisica, Università di Trento, 38123 Povo, Italy*

(Received 27 October 2021; revised 27 May 2022; accepted 2 June 2022; published 17 June 2022)

Since the realization of high-quality microwave cavities coupled to quantum dots, one can envisage the possibility to investigate the coherent interaction of light and matter in semiconductor quantum devices. Here we study a parallel double quantum dot device operating as single-electron splitter interferometer, with each dot coupled to a local photon cavity. We explore, how quantum correlation and entanglement between the two separated cavities are generated by the coherent transport of a single electron passing simultaneously through the two different dots. We calculate the covariance of the cavity occupations by using a diagrammatic perturbative expansion based on Keldysh Green's functions to fourth order in the dot-cavity interaction strength, taking into account vertex diagrams. Furthermore, we demonstrate the creation of entanglement by showing that the classical Cauchy-Schwarz inequality is violated if the energy levels of the two dots are almost degenerate. For large level detuning or a single dot coupled to two cavities, we show that the inequality is not violated.

DOI: 10.1103/PhysRevB.105.L241407

I. INTRODUCTION

Nonlocality is a fundamental property of quantum mechanics that manifests in two main ways: as delocalization of a quantum particle in space according to its associated wave function (superposition) and as correlations between spatially separated parts of a quantum system (entanglement). It is at the heart of quantum communication and computing in various physical implementations.

An intriguing example of quantum delocalization is interference in the motion of a single electron. Quantum delocalized transport has been proven in nanodevices formed by two possible paths connecting an initial point and a final point, namely, two electrical contacts playing the role of source and drain. Examples are parallel double dots [1–3], operating as a single-electron splitter interferometer, and the electronic Mach-Zehnder interferometer [4], operating with the edge states of two-dimensional quantum Hall systems [5]. Similar to a photon in a Mach-Zehnder interferometer, an electron wave function can split in two branches and then, by recombining, can give rise to interference in the transmitted flux. In general, semiconducting single-electron devices form a unique playground to address nonlocal electron transport and quantum interference [1–3,6,7].

Besides electron transport, quantum mechanics can be explored with high precision in the fields of optics and photonics. In particular, microwave quantum photonics has made remarkable progress in the last decade. In the circuit quantum electrodynamics (QED) architecture [8], a large variety of quantum states in an electromagnetic microwave resonator have been prepared and measured [9,10]. Moreover, using superconducting qubits or Josephson circuitry (Josephson parametric amplifier or wave mixer), quantum entangled states of microwave photons have been realized in two spatially separated resonator cavities [11], in two resonator modes of different frequencies [12,13], and in propagating photons [14–16]. More recently, an entangled pair of two-mode cat states was realized in two microwave cavities [17], and a dc-biased Josephson junction was used to create two continuous entangled microwave beams [18].

Beyond superconducting circuits based on Josephson junctions, quantum dots realized in semiconducting nanostructures implement reliable and well-controlled qubits [19,20] with transition frequencies in the microwave domain and with the advantage of electric field control [21]. Quantum dots can now be readily coupled to microwave photon cavities, leading to the field of semiconductor hybrid QED [22], which provides a novel family of coherent quantum devices that combine electronic with photonic degrees of freedom on chip [23–33]. The so-called strong-coupling regime has been reached [34–36], along with the full microwave control and readout of the quantum dot qubits [37].

Coupling quantum dots with quantum optical resonators adds a new dimension to the cavity and circuit QED, beyond the conventional paradigm of an atom coupled to a harmonic oscillator. This research line opens the path to exploring the correlations between charge transport and nonequilibrium, possibly quantum, regimes of localized electromagnetic radiation. The corresponding hybrid devices are promising for implementing quantum transducers, in which single electrons control photonic quantum states in microwave cavities.

II. THE SYSTEM

In this context, we analyze a parallel double quantum dot system, as shown in Fig. 1(a), with each dot capacitively

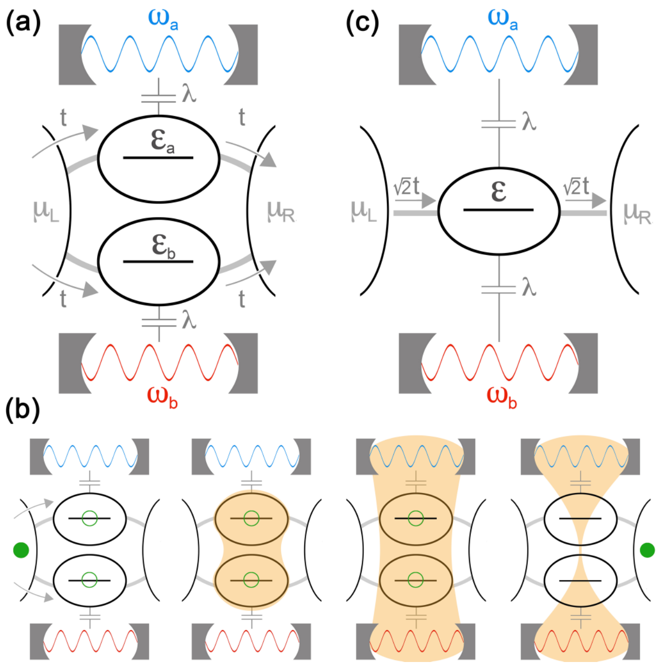

FIG. 1. Sketch of the studied systems and idea. (a) Main model: a parallel double quantum dot with a single electronic energy level in each quantum dot. Each dot is coupled to one of two separated microwave cavities and common left and right leads. (b) Basic idea: An electron travels through both branches of the parallel double quantum dot simultaneously. Its state is a coherent superposition of the states in the two dots. The delocalization of the single electron yields quantum correlations between the two cavities and remains even when the electron leaves the system. (c) Single quantum dot with a single electronic energy level coupled to two microwave cavities.

coupled to one of two separated microwave cavities of resonance frequencies ω_a and ω_b. The two dots are connected to common left and right leads with the same hopping parameter t. We denote the coupling strength of the dot-cavity interaction by λ.

We study a spinless model, consisting of a single electron state in each dot, whose energy level is given by $\varepsilon_{a,b} = \bar{\varepsilon} \pm \Delta\varepsilon$ for the upper and lower dots, respectively. There is no direct tunneling between the dots. *A priori*, we cannot exclude the possibility that both dots are occupied simultaneously. However, the tunneling of electrons into the double-dot system is an uncorrelated event in our model due to the lack of electron-electron interactions. The process itself therefore cannot generate quantum correlations between the two microwave cavities that go beyond the elementary single-electron tunneling process that we discuss in the following.

We explore how correlation and entanglement between the two cavities emerge through the coherent transport of a single electron passing simultaneously through the two different dots. Let us first assume that the energy levels of the dots are close to each other in the sense that the energy difference is small compared to their broadening $|\Delta\varepsilon| = |\varepsilon_a - \varepsilon_b| \ll \Gamma$, i.e., the energy distributions overlap. In this regime the two paths are indistinguishable, and the electron flows through both branches simultaneously, causing quantum interference in the double quantum dot system. This means that the linear conductance associated with the levels of the double dot system is different from the sum of the linear conductances of the two separate dots, i.e., different from the single-level regime.

If the difference between the two energy levels is increased, i.e., $|\Delta\varepsilon| \gg \Gamma$, the interference is destroyed, and the electron transfer occurs via the incoherent sum of the two possible paths; namely, the electron proceeds independently through the upper or lower branch but not simultaneously through both. This is the mechanism that allows or prevents entanglement.

As illustrated in Fig. 1(b), the idealized procedure is as follows: When the electron travels inside the system, it splits. Therefore, the electronic state is a coherent superposition of the electron occupying the upper dot or the lower dot, with the corresponding occupations $n_a^{(el)}$ and $n_b^{(el)}$. The state of the complete system is this superposed electron state coupled to the two ground states of the cavities $|GS\rangle_a$ and $|GS\rangle_b$:

$$|\Psi\rangle_{in} = \frac{1}{\sqrt{2}}\Big(\big|n_a^{(el)} = 1, n_b^{(el)} = 0\big\rangle + \big|n_a^{(el)} = 0, n_b^{(el)} = 1\big\rangle\Big)|GS\rangle_a|GS\rangle_b. \quad (1)$$

The interaction between an electron in a dot and the corresponding cavity ensures that a coherent state is created, depending on the position of the electron, described by the unitary time evolution operator

$$\hat{U}(\tau) = \hat{\mathcal{D}}_a\big[\hat{n}_a^{(el)}\rho(\tau)\big] \times \hat{\mathcal{D}}_b\big[\hat{n}_b^{(el)}\rho(\tau)\big], \quad (2)$$

where $\hat{\mathcal{D}}_{a,b}[\xi]$ are the coherent displacement operators with the associated parameter ξ and $\rho(t) = -i\lambda t$. (We set $\hbar = 1$ here and in the following.) After some dwell time τ the state has evolved, and the dot-cavity interaction correlates the two cavities,

$$U(\tau)|\Psi\rangle_{in} = \frac{1}{\sqrt{2}}\Big(\big|n_a^{(el)} = 1, n_b^{(el)} = 0\big\rangle|\rho(\tau)\rangle_a|GS\rangle_b + \big|n_a^{(el)} = 0, n_b^{(el)} = 1\big\rangle|GS\rangle_a|\rho(\tau)\rangle_b\Big), \quad (3)$$

where $|\rho(\tau)\rangle_a$ and $|\rho(\tau)\rangle_b$ are coherent states of the cavities. The quantum delocalization of the single electron in the double dot leads to a quantum correlation of the two cavities, which indicates the possibility of an entangled state. This state can persist even when the electron leaves the system and the dot state is empty,

$$|\Psi\rangle_{out} = \frac{1}{\sqrt{2}}|0,0\rangle\big(|\rho(\tau)\rangle_a|GS\rangle_b + |GS\rangle_a|\rho(\tau)\rangle_b\big). \quad (4)$$

Notice that in the last step the electron is removed without the knowledge of which path it passed through, and this operation corresponds to a kind of nonlocal measurement.

When a second electron subsequently enters the double dot, one can repeat a similar argument starting from the entangled photon state instead of the vacuum. However, for long times, the internal losses of the cavities should be included, along with their energy relaxation and dephasing due to the coupling with the conducting leads via the double dot. In other words, Fig. 1(b) describes just the idealized argument of the entanglement generation process, where it is assumed that the interaction time of the electron and the cavity is short and that decoherence effects of the dots happen much later regarding the timescale of the interaction.

To investigate the possibility of entanglement, we will evaluate two quantities: We prove correlation via the covariance of the Fock occupation numbers and quantum correlation via the violation of the classical Cauchy-Schwarz inequality [38] for the two cavities. We calculate these quantities using a perturbative expansion in the Keldysh Green's function formalism. To understand the underlying mechanism of the entanglement generation, we compare the results of the double quantum dot system for degenerate levels, namely, zero-energy difference of the two levels, with those of a large energy level difference. In addition, we discuss the results for a single quantum dot coupled to two cavities with the same dot-cavity coupling constant λ but with a dot-lead tunneling coupling of $\sqrt{2}t$ [see Fig. 1(c)].

III. THEORETICAL MODEL

A. Basic formalism

The double quantum dot system with the attached cavities is described by the following Hamiltonian including the electronic and photonic parts as well as the electron-photon interaction:

$$\hat{H} = \hat{H}_{\mathrm{el}} + \hat{H}_{\mathrm{ph}} + \hat{H}_{\mathrm{int}}, \tag{5}$$

$$\hat{H}_{\mathrm{el}} = \sum_{r=\mathrm{L,R}} \sum_{k} (\varepsilon_{kr} - \mu_r)\hat{c}^{\dagger}_{kr}\hat{c}_{kr} + \sum_{\alpha=\mathrm{a,b}} \varepsilon_\alpha \hat{d}^{\dagger}_{\alpha}\hat{d}_\alpha + t \sum_{r=\mathrm{L,R}} \sum_{\alpha=\mathrm{a,b}} \sum_{k} (\hat{c}^{\dagger}_{kr}\hat{d}_\alpha + \mathrm{H.c.}), \tag{6}$$

$$\hat{H}_{\mathrm{ph}} = \sum_{\alpha=\mathrm{a,b}} \omega_\alpha \hat{\alpha}^{\dagger}\hat{\alpha}, \tag{7}$$

$$\hat{H}_{\mathrm{int}} = \lambda \sum_{\alpha=\mathrm{a,b}} (\hat{\alpha}^{\dagger} + \hat{\alpha})\hat{d}^{\dagger}_{\alpha}\hat{d}_\alpha. \tag{8}$$

In this work we focus on the noninteracting, spinless model for the electronic system [39,40]. We disregard the spin degree of freedom because the interaction with the cavity is spin independent. The electron spin is therefore not crucial for the entanglement generation process that we focus on here. $\hat{c}^{\dagger}_{kr}$ and $\hat{d}^{\dagger}_{\alpha}$, with $r = \mathrm{L,R}$ and $\alpha = \mathrm{a,b}$, are the creation operators of the electrons in the left and right leads and in the two quantum dots with energy levels ε_α. $\hat{\alpha}^{\dagger}$ and $\hat{\alpha}$ are the creation and annihilation operators of photons with frequency ω_α in cavity α. $t \in \mathbb{R}$ is the hopping parameter describing the transport of an electron between dots and leads.

We focus on the regime of unidirectional transport. The voltage that is applied along the system shifts the electrochemical potentials of the leads. We consider a symmetric shift in the high-voltage limit

$$\mu_{\mathrm{L}} = -\mu_{\mathrm{R}} = \lim_{eV\to\infty} eV/2. \tag{9}$$

The Fermi functions of the left and right leads become $f_{\mathrm{L}}(E) = 1$ and $f_{\mathrm{R}}(E) = 0$. This approximation holds as long as the potential is the largest energy scale involved in our model, namely, $|eV| \gg \max(k_{\mathrm{B}}T, \Gamma, \Delta\varepsilon, \omega_0, \eta)$. Here $k_{\mathrm{B}}T$ is the temperature of the leads, and η is the damping parameter, characterizing the cavity losses (see below). The origin of the dot energy levels is chosen to be in the middle of the electrochemical potentials of the two leads, i.e., $\bar{\varepsilon} = 0$. Dot energies are therefore specified by the level difference, i.e., $\varepsilon_{\mathrm{a,b}} = \pm\Delta\varepsilon$.

Let us note that we assume identical dot-lead couplings in Eq. (6). If dot levels are degenerate, $\Delta\varepsilon = 0$, and dot-electrode couplings differ, the transmission function typically shows a dip at energies in close vicinity to $\bar{\varepsilon}$ instead of the peak arising at all identical couplings. We explain in the Supplemental Material [41] why a small asymmetry in electrode-dot couplings is not expected to affect our main results. The essential argument is that since we are assuming the high-voltage limit, a local singularity of transport properties at $\bar{\varepsilon}$ is averaged out. The singularity thus does not lead to a discontinuous behavior of the integral of the total electron flux or any other quantities, like Feynman diagrams, derived from integrals over energy [42].

To determine the electronic transport through the system in the absence of electron-photon interaction, we calculate the unperturbed electronic Green's functions associated with the electronic part $\hat{H}_{\mathrm{el}}$ of the Hamiltonian, using the diagrammatic Keldysh technique and applying the wideband approximation for the leads [43,44]. In this way we obtain the broadening Γ of the electronic levels. These electronic Green's functions represent our bare propagators in the perturbative approach, where we expand in terms of the electron-photon interaction. These unperturbed fermionic Green's functions $G_{\alpha\beta}(t_i, t_j) = -i\langle T_{\mathrm{c}}(\hat{d}_\alpha(t)\hat{d}^{\dagger}_{\beta}(t'))\rangle$, beyond being in the matrix form of the Keldysh formalism [45], can also be brought into the form of 2×2 matrices related to the two parallel dots $\alpha, \beta = \mathrm{a,b}$ [44]. T_{c} is the time-ordering operator with respect to the Keldysh contour. In a similar way, we define the single-particle bosonic Green's function $D_\alpha(t, t') = -i\langle T_{\mathrm{c}}(\hat{\alpha}(t)\hat{\alpha}^{\dagger}(t'))\rangle$ for the two cavities and the two-particle function $F_{\alpha\beta}(t, t') = -i\langle T_{\mathrm{c}}(\hat{\alpha}(t)\hat{\beta}(t)\hat{\alpha}^{\dagger}(t')\hat{\beta}^{\dagger}(t'))\rangle$. We consider the intrinsic photon losses in the two cavities using a finite broadening η of the unperturbed bosonic propagators, denoted as $D^{(0)}_{\alpha}(t, t')$. The explicit form of the unperturbed Green's functions is detailed in the Supplemental Material, Sec. A [41].

To demonstrate the entanglement of photons in the two cavities, we calculate the covariance

$$C = \langle \hat{n}_{\mathrm{a}}\hat{n}_{\mathrm{b}}\rangle - \langle \hat{n}_{\mathrm{a}}\rangle\langle \hat{n}_{\mathrm{b}}\rangle, \tag{10}$$

which proves correlation if it is finite, i.e., $C \neq 0$, and test the classical Cauchy-Schwarz inequality

$$S = \frac{\langle \hat{a}^{\dagger}\hat{a}\hat{b}^{\dagger}\hat{b}\rangle}{\sqrt{\langle \hat{a}^{\dagger}\hat{a}^{\dagger}\hat{a}\hat{a}\rangle}\sqrt{\langle \hat{b}^{\dagger}\hat{b}^{\dagger}\hat{b}\hat{b}\rangle}} \leqslant 1, \tag{11}$$

which proves quantum correlation if it is violated. The cavity occupations are defined by the bosonic creation and annihilation operators $\hat{n}_{\mathrm{a}} = \hat{a}^{\dagger}\hat{a}$ and $\hat{n}_{\mathrm{b}} = \hat{b}^{\dagger}\hat{b}$, and S is the Cauchy-Schwarz parameter.

To evaluate Eqs. (10) and (11), we express the expectation values by Keldysh Green's functions and perform a diagrammatic perturbative expansion in the dot-cavity coupling λ up to fourth order. The expectation values in these equations are related to the lesser Green's functions in the limit of equal times of the single-particle and two-particle Green's functions [45]. In this representation, the average photon number of a single cavity $\langle\hat{n}_\alpha\rangle$, the covariance C, and the Cauchy-Schwarz parameter S read

$$\langle\hat{n}_\alpha\rangle = D^<_\alpha(t,t), \tag{12}$$

$$C = iF^<_{\text{ab}}(t,t) + D^<_{\text{a}}(t,t)D^<_{\text{b}}(t,t), \tag{13}$$

$$S = \frac{F^<_{\text{ab}}(t,t)}{\sqrt{F^<_{\text{aa}}(t,t)F^<_{\text{bb}}(t,t)}}. \tag{14}$$

The conditions for entanglement are a nonzero covariance, $C \neq 0$, and a violated classical Cauchy-Schwarz inequality, i.e., $S > 1$. Both quantities have no finite contributions up to third order, so we have to calculate them consistently up to fourth order in λ.

B. Perturbation expansion

For the single-particle bosonic Green's functions in Eqs. (12) and (13) we perform a perturbation expansion up to second order, and for the two-particle Green's function in Eqs. (13) and (14) we perform one up to fourth order with respect to the dot-cavity interaction Hamiltonian in the interaction picture,

$$H_{\text{int}}(\tau) = \lambda[(\hat{a}^\dagger + \hat{a})\hat{d}^\dagger_{\text{a}}\hat{d}_{\text{a}} + (\hat{b}^\dagger + \hat{b})\hat{d}^\dagger_{\text{b}}\hat{d}_{\text{b}}]_\tau. \tag{15}$$

To calculate the expectation values we use Wick's theorem, which allows us to decompose a contour-ordered string of creation and annihilation operators into a sum over all possible pairwise products [45].

Every product corresponds to unperturbed fermionic $G_{\alpha\beta}(t_i,t_j)$ and bosonic Green's functions $D^{(0)}_\alpha(t_i,t_j)$, with t_i and t_j lying on the Keldysh contour. An expansion up to fourth order yields contributions with four bosonic and four fermionic Green's functions, integrated over four different time arguments distributed on the Keldysh contour. As an example we consider the integral

$$\begin{aligned} I(t,t') = \lambda^4 \oint_c \oint_c \oint_c \oint_c dt_1 dt_2 dt_3 dt_4 \\ \times D^{(0)}_{\text{a}}(t,t_1)D^{(0)}_{\text{b}}(t_2,t')D^{(0)}_{\text{b}}(t,t_3)D^{(0)}_{\text{a}}(t_4,t') \\ \times G_{\text{ab}}(t_4,t_3)G_{\text{ba}}(t_3,t_4)G_{\text{ab}}(t_1,t_2)G_{\text{ba}}(t_2,t_1), \end{aligned} \tag{16}$$

which contributes to the covariance and the classical Cauchy-Schwarz parameter. We can represent these integrals as Feynman diagrams and get three different geometries, as depicted in Fig. 2, while the latter equation corresponds to the third diagram. Due to the fourth order of the perturbative expansion we get four interaction points proportional to λ. This shows that we are dealing with a two-photon process, emitting and absorbing photons in both cavities a and b with corresponding energies $\omega_{\text{a,b}}$. The process is described by different types of fermionic interaction in the double quantum dot system. Complete formulas for C and S are reported in the Supplemental Material, Sec. B [41].

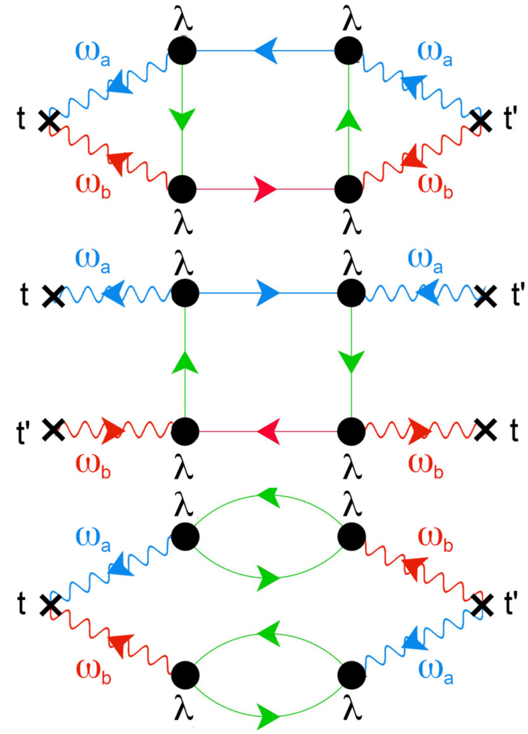

FIG. 2. Examples of vertex diagrams, which contribute to the integrals of C and S. Black dots represent the electron-photon interaction proportional to λ. Wiggly lines correspond to bosonic Green's functions of the microwave cavities with resonance frequency $\omega_{\text{a,b}}$, distinguished by the colors red and blue. Straight lines signify fermionic Green's functions of the double quantum dot system. Diagonal Green's functions are indicated by blue and red lines; off-diagonal Green's functions are represented in green.

IV. RESULTS

To certain limits, we are able to calculate the relevant quantities analytically. We consider equal resonance frequencies $\omega_{\text{a}} = \omega_{\text{b}} \equiv \omega_0$ and zero temperature of the cavities. Furthermore, we focus on the regime of low damping inside the cavities, i.e., $\omega_0 \gg \Gamma \gg \eta$, and on the high-voltage bias limit. Regarding the energy levels of the parallel quantum dots we consider two different cases: First, we study the case of two almost equal energy levels, and second, we study the case for two strongly differing levels. Finally, we compare these results with the case of a single dot coupled to two cavities at the same time [see Fig. 1(c)].

We first determine the average photon number of the single cavities $\langle\hat{n}_{\text{a}}\rangle = \langle\hat{n}_{\text{b}}\rangle = \bar{n}$ up to second order and the corresponding fluctuations $\delta n^2 = \langle\hat{n}^2\rangle - \bar{n}^2$ up to fourth order. The latter quantity can be easily computed from the knowledge of $\bar{n}$ and $\langle\hat{\alpha}^\dagger\hat{\alpha}^\dagger\hat{\alpha}\hat{\alpha}\rangle$ [namely, $F^<_{\alpha\alpha}(t,t)$]. Then we can analyze the behavior of the Fano factor, defined as $F = \delta n^2/\bar{n}$. Finally, we calculate the covariance C and the Cauchy-Schwarz parameter S both up to fourth order in λ. Due to the symmetries in the system, the results for both cavities are the same. The average occupations for the single dot and the double dot with large level spacing are equal since we calculate the average occupation up to only second order. The result of the double dot with two almost equal energy levels, i.e., $\Delta\varepsilon \ll \Gamma$, acting

TABLE I. Results for the average photon number of a single cavity $\bar{n}$, fluctuations δn^2, Fano factor F, covariance C, and Cauchy-Schwarz parameter S for three different cases: the double quantum dot (DQD) with zero or large level spacing and a single quantum dot coupled to two cavities. Here $n_0 = \pi^2\left(\frac{\lambda}{\omega_0}\right)^2\left(\frac{\Gamma}{\eta}\right)$.

	DQD, $\Delta\varepsilon = 0$	DQD, $\Delta\varepsilon \gg \Gamma$	Single dot
$\bar{n}$	n_0	$2n_0$	$2n_0$
δn^2	$n_0(1 - n_0/4)$	$2n_0(1 + n_0)$	$2n_0(1 + 4n_0)$
F	$1 - n_0/4$	$1 + n_0$	$1 + 4n_0$
C	$n_0^2/2$	0	$8n_0^2$
S	2	2/3	1

as a single-electron splitter, is half the size of the case $\Delta\varepsilon \gg \Gamma$ and the single-dot system. In the case of zero or small level spacing the electronic Hamiltonian, Eq. (6), can be written in the form of an effective single-dot problem. Compared to the real single-dot case the dot-lead coupling parameter t is renormalized to $t \to t/\sqrt{2}$. With $\Gamma \propto |t|^2$ this renormalization enters as a factor of 2 in the bosonic occupation of the cavities [44]. Furthermore, we checked that the result for the single dot coupled simultaneously to two cavities coincides with previous results in the limit, in which the induced damping associated with the electron-boson interaction is smaller than the intrinsic damping of the cavities η [46,47].

According to Table I, for the fluctuations and the corresponding Fano factor of the double-dot system we find a sub-Poissonian behavior in the regime, where we have quantum interference in the transport through the double dot, whereas we obtain a super-Poissonian behavior for the other two cases. The sub-Poissonian behavior corresponds to a photon antibunching in the local cavity. Let us emphasize that the nature of the interaction already appears at the level of a single-cavity quantity, namely, the local fluctuations of the photons in a cavity. This can also be seen for two trivial examples since the sub-Poissonian behavior occurs both for the entangled bosonic states in the Fock occupation $|\Psi\rangle_{pq} \propto |n_\mathrm{a} = p, n_\mathrm{b} = q\rangle + |n_\mathrm{a} = q, n_\mathrm{b} = p\rangle$, with $p, q \in \mathbb{N}$, and in the coherent state basis $|\Psi\rangle_{z_1 z_2} \propto |\xi_\mathrm{a} = z_1, \xi_\mathrm{b} = z_2\rangle + |\xi_\mathrm{a} = z_2, \xi_\mathrm{b} = z_1\rangle$, with $|\xi\rangle$ being a coherent state and $z_1, z_2 \in \mathbb{C}$.

For the covariance C we find a finite, positive value for the double quantum dot with two equal energy levels, which verifies the correlation of the photons in the single cavities. The covariance for a large level spacing vanishes, meaning that there is no correlation. This result is expected for the case of two separated electron pathways. Notice, however, that finite covariance also arises in the case of a single dot simultaneously coupled to two cavities [see Fig. 1(c)]. This can be interpreted as a classical correlation, as we have a single-photon emitter coupled to both cavities.

Finite covariance proves correlation but does not indicate quantum correlation (entanglement). To distinguish classical and quantum correlations, we calculated the classical Cauchy-Schwarz parameter S in Eq. (14), which we cast in the following form:

$$S = \frac{|\bar{n}^2 + C|}{|\bar{n}(\bar{n} - 1) + \delta n^2|} = \frac{\left|\bar{n} + \frac{C}{\bar{n}}\right|}{|\bar{n} + F - 1|}. \tag{17}$$

The expression states that a violated Cauchy-Schwarz inequality ($S > 1$) occurs if a finite and positive covariance is combined with a sub-Poissonian ($F < 1$) behavior. As reported in Table I, the Cauchy-Schwarz inequality for vanishing level spacing is clearly violated. This confirms the quantum entanglement of the photons in the two distant microwave cavities if the energy levels of the two dots are sufficiently close to each other, viz., the electron is delocalized over the two dots when it flows from one lead to the other. For strongly differing energy levels of the dots, the classical Cauchy-Schwarz inequality is no longer violated as $C = 0$ (uncorrelated systems). As a sanity check, for the single dot with $C > 0$ and $F > 1$ (super-Poissonian) we find that the classical Cauchy-Schwarz inequality is not violated but reaches the maximum classical value.

Let us finally discuss the role of decoherence in the system. Intrinsic contributions stem from losses in the cavities. Therefore, we assume high-quality cavities with an intrinsic damping that is smaller than the broadening of the electronic levels $\eta \ll \Gamma \ll \omega_0$. We expect the photon production rate to be proportional to the flow of electrons through the dots. If the cavities lose energy at a rate which is faster than the rate at which photons are created, this will, of course, destroy entanglement. Another source of decoherence arises from the stochastic nature of electron tunneling. The granular electron flow cannot generate a pure quantum state of the photons in the two cavities, but it will create an entangled mixed state.

We propose our setup as a proof of concept to realize bosonic quantum correlations mediated by single-electron transport. Although several parameters were assumed to be equal, we expect our results to be relevant for carefully chosen experimental settings. Since the covariance C and the Cauchy-Schwarz parameter S are continuous functions of the parameters of the Hamiltonian, we expect our idealized proposal to be robust to small variations and hence to be realizable. A long-term perspective may be the creation of pure entangled states. For this objective time-dependent control of electron occupations of the dots may need to be implemented along the lines discussed in [9,10].

V. SUMMARY

We studied single-electron transport through a parallel double quantum dot, with each dot being coupled to a separate microwave cavity. We showed in a simple scheme that for degenerate dot energies, when quantum interference between the two transport pathways is most pronounced, the delocalized electron entangles the photons in two separated microwave cavities. Using the Keldysh Green's function method and a perturbative expansion up to fourth order in the dot-cavity interaction strength, we demonstrated quantum correlations between the cavities through nonzero covariance and the violation of the classical Cauchy-Schwarz inequality. Due to the complexity of the calculations we presented analytical results only for the perfectly symmetric case, with both quantum dots exhibiting equal energy levels. But we expect that our findings are still valid if the degeneracy is lifted and the system becomes slightly asymmetric. For too large level detunings or a single dot coupled to two cavities, we have shown that the photons in the different cavities cannot be entangled.

ACKNOWLEDGMENTS

This work was supported by the Deutsche Forschungsgemeinschaft (DFG, German Research Foundation) through Project No. 32152442 - SFB 767 and Project No. 25217212 - SFB 1432 and by the German Excellence Strategy via the Zukunftskolleg of the University of Konstanz.

[1] A. W. Holleitner, C. R. Decker, H. Qin, K. Eberl, and R. H. Blick, Coherent Coupling of Two Quantum Dots Embedded in an Aharonov-Bohm Interferometer, Phys. Rev. Lett. **87**, 256802 (2001).

[2] M. Sigrist, T. Ihn, K. Ensslin, M. Reinwald, and W. Wegscheider, Coherent Probing of Excited Quantum Dot States in an Interferometer, Phys. Rev. Lett. **98**, 036805 (2007).

[3] T. Hatano, T. Kubo, Y. Tokura, S. Amaha, S. Teraoka, and S. Tarucha, Aharonov-Bohm Oscillations Changed by Indirect Interdot Tunneling via Electrodes in Parallel-Coupled Vertical Double Quantum Dots, Phys. Rev. Lett. **106**, 076801 (2011).

[4] G. Haack, H. Förster, and M. Büttiker, Parity detection and entanglement with a Mach-Zehnder interferometer, Phys. Rev. B **82**, 155303 (2010).

[5] Y. Ji, Y. Chung, D. Sprinzak, M. Heiblum, D. Mahalu, and H. Shtrikman, An electronic Mach–Zehnder interferometer, Nature (London) **422**, 415 (2003).

[6] R. Schuster, E. Buks, M. Heiblum, D. Mahalu, V. Umansky, and H. Shtrikman, Phase measurement in a quantum dot via a double-slit interference experiment, Nature (London) **385**, 417 (1997).

[7] E. Bocquillon, V. Freulon, J. M. Berroir, P. Degiovanni, B. Plaçais, A. Cavanna, Y. Jin, and G. Fève, Coherence and indistinguishability of single electrons emitted by independent sources, Science **339**, 1054 (2013).

[8] A. Blais, A. L. Grimsmo, S. M. Girvin, and A. Wallraff, Circuit quantum electrodynamics, Rev. Mod. Phys. **93**, 025005 (2021).

[9] M. Hofheinz, E. M. Weig, M. Ansmann, R. C. Bialczak, E. Lucero, M. Neeley, A. D. O'Connell, H. Wang, J. M. Martinis, and A. N. Cleland, Generation of Fock states in a superconducting quantum circuit, Nature (London) **454**, 310 (2008).

[10] M. Hofheinz, H. Wang, M. Ansmann, R. C. Bialczak, E. Lucero, M. Neeley, A. D. O'Connell, D. Sank, J. Wenner, J. M. Martinis, and A. N. Cleland, Synthesizing arbitrary quantum states in a superconducting resonator, Nature (London) **459**, 546 (2009).

[11] H. Wang, M. Mariantoni, R. C. Bialczak, M. Lenander, E. Lucero, M. Neeley, A. D. O'Connell, D. Sank, M. Weides, J. Wenner, T. Yamamoto, Y. Yin, J. Zhao, J. M. Martinis, and A. N. Cleland, Deterministic Entanglement of Photons in Two Superconducting Microwave Resonators, Phys. Rev. Lett. **106**, 060401 (2011).

[12] E. Zakka-Bajjani, F. Nguyen, M. Lee, L. R. Vale, R. W. Simmonds, and J. Aumentado, Quantum superposition of a single microwave photon in two different 'colour' states, Nat. Phys. **7**, 599 (2011).

[13] F. Nguyen, E. Zakka-Bajjani, R. W. Simmonds, and J. Aumentado, Quantum Interference between Two Single Photons of Different Microwave Frequencies, Phys. Rev. Lett. **108**, 163602 (2012).

[14] C. Eichler, D. Bozyigit, C. Lang, M. Baur, L. Steffen, J. M. Fink, S. Filipp, and A. Wallraff, Observation of Two-Mode Squeezing in the Microwave Frequency Domain, Phys. Rev. Lett. **107**, 113601 (2011).

[15] E. Flurin, N. Roch, F. Mallet, M. H. Devoret, and B. Huard, Generating Entangled Microwave Radiation over Two Transmission Lines, Phys. Rev. Lett. **109**, 183901 (2012).

[16] C. Lang, C. Eichler, L. Steffen, J. M. Fink, M. J. Woolley, A. Blais, and A. Wallraff, Correlations, indistinguishability and entanglement in Hong–Ou–Mandel experiments at microwave frequencies, Nat. Phys. **9**, 345 (2013).

[17] C. Wang, Y. Y. Gao, P. Reinhold, R. W. Heeres, N. Ofek, K. Chou, C. Axline, M. Reagor, J. Blumoff, K. M. Sliwa, L. Frunzio, S. M. Girvin, L. Jiang, M. Mirrahimi, M. H. Devoret, and R. J. Schoelkopf, A Schrödinger cat living in two boxes, Science **352**, 1087 (2016).

[18] A. Peugeot, G. Ménard, S. Dambach, M. Westig, B. Kubala, Y. Mukharsky, C. Altimiras, P. Joyez, D. Vion, P. Roche, D. Esteve, P. Milman, J. Leppäkangas, G. Johansson, M. Hofheinz, J. Ankerhold, and F. Portier, Generating Two Continuous Entangled Microwave Beams Using a dc-Biased Josephson Junction, Phys. Rev. X **11**, 031008 (2021).

[19] J. R. Petta, A. C. Johnson, J. M. Taylor, E. A. Laird, A. Yacoby, M. D. Lukin, C. M. Marcus, M. P. Hanson, and A. C. Gossard, Coherent manipulation of coupled electron spins in semiconductor quantum dots, Science **309**, 2180 (2005).

[20] F. H. L. Koppens, C. Buizert, K. J. Tielrooij, I. T. Vink, K. C. Nowack, T. Meunier, L. P. Kouwenhoven, and L. M. K. Vandersypen, Driven coherent oscillations of a single electron spin in a quantum dot, Nature (London) **442**, 766 (2006).

[21] K. C. Nowack, F. H. L. Koppens, Y. V. Nazarov, and L. M. K. Vandersypen, Coherent control of a single electron spin with electric fields, Science **318**, 1430 (2007).

[22] G. Burkard, M. J. Gullans, X. Mi, and J. R. Petta, Superconductor–semiconductor hybrid-circuit quantum electrodynamics, Nat. Rev. Phys. **2**, 129 (2020).

[23] K. D. Petersson, L. W. McFaul, M. D. Schroer, M. Jung, J. M. Taylor, A. A. Houck, and J. R. Petta, Circuit quantum electrodynamics with a spin qubit, Nature (London) **490**, 380 (2012).

[24] C. Rössler, D. Oehri, O. Zilberberg, G. Blatter, M. Karalic, J. Pijnenburg, A. Hofmann, T. Ihn, K. Ensslin, C. Reichl, and W. Wegscheider, Transport Spectroscopy of a Spin-Coherent Dot-Cavity System, Phys. Rev. Lett. **115**, 166603 (2015).

[25] J. J. Viennot, M. C. Dartiailh, A. Cottet, and T. Kontos, Coherent coupling of a single spin to microwave cavity photons, Science **349**, 408 (2015).

[26] L. E. Bruhat, J. J. Viennot, M. C. Dartiailh, M. M. Desjardins, T. Kontos, and A. Cottet, Cavity Photons as a Probe for Charge Relaxation Resistance and Photon Emission in a Quantum Dot Coupled to Normal and Superconducting Continua, Phys. Rev. X **6**, 021014 (2016).

[27] D. Hagenmüller, S. Schütz, J. Schachenmayer, C. Genes, and G. Pupillo, Cavity-assisted mesoscopic transport of fermions:

Coherent and dissipative dynamics, Phys. Rev. B **97**, 205303 (2018).

[28] M. Trif and P. Simon, Braiding of Majorana Fermions in a Cavity, Phys. Rev. Lett. **122**, 236803 (2019).

[29] W. Khan, P. Potts, S. Lehmann, K. Thelander, C. Dick, P. Samuelsson, and V. Maisi, Efficient and continuous microwave photoconversion in hybrid cavity-semiconductor nanowire double quantum dot diodes, Nat. Commun. **12**, 5130 (2021).

[30] A. Cottet, Z. Leghtas, and T. Kontos, Theory of interactions between cavity photons induced by a mesoscopic circuit, Phys. Rev. B **102**, 155105 (2020).

[31] O. Dmytruk, M. Trif, C. Mora, and P. Simon, Out-of-equilibrium quantum dot coupled to a microwave cavity, Phys. Rev. B **93**, 075425 (2016).

[32] J. Lu, R. Wang, J. Ren, M. Kulkarni, and J.-H. Jiang, Quantum-dot circuit-QED thermoelectric diodes and transistors, Phys. Rev. B **99**, 035129 (2019).

[33] B. Bhandari, P. A. Erdman, R. Fazio, E. Paladino, and F. Taddei, Thermal rectification through a nonlinear quantum resonator, Phys. Rev. B **103**, 155434 (2021).

[34] X. Mi, J. V. Cady, D. M. Zajac, P. W. Deelman, and J. R. Petta, Strong coupling of a single electron in silicon to a microwave photon, Science **355**, 156 (2016).

[35] A. Stockklauser, P. Scarlino, J. V. Koski, S. Gasparinetti, C. K. Andersen, C. Reichl, W. Wegscheider, T. Ihn, K. Ensslin, and A. Wallraff, Strong Coupling Cavity QED with Gate-Defined Double Quantum Dots Enabled by a High Impedance Resonator, Phys. Rev. X **7**, 011030 (2017).

[36] X. Mi, M. Benito, S. Putz, D. M. Zajac, J. M. Taylor, G. Burkard, and J. R. Petta, A coherent spin–photon interface in silicon, Nature (London) **555**, 599 (2018).

[37] P. Scarlino, D. J. van Woerkom, A. Stockklauser, J. V. Koski, M. C. Collodo, S. Gasparinetti, C. Reichl, W. Wegscheider, T. Ihn, K. Ensslin, and A. Wallraff, All-Microwave Control and Dispersive Readout of Gate-Defined Quantum Dot Qubits in Circuit Quantum Electrodynamics, Phys. Rev. Lett. **122**, 206802 (2019).

[38] S. Wölk, M. Huber, and O. Gühne, Unified approach to entanglement criteria using the Cauchy-Schwarz and Hölder inequalities, Phys. Rev. A **90**, 022315 (2014).

[39] In contrast, when interdot Coulomb interaction is included, the two levels exhibit an energy splitting renormalization that scales logarithmically with the Coulomb energy, even for the spinless fermion model. This subject was studied in Ref. [40].

[40] D. Boese, W. Hofstetter, and H. Schoeller, Interference and interaction effects in multilevel quantum dots, Phys. Rev. B **64**, 125309 (2001).

[41] See Supplemental Material at http://link.aps.org/supplemental/10.1103/PhysRevB.105.L241407 for the explicit formulas of the Green's functions, for the derivation of the perturbation expansion and the construction of the diagrams, and for a discussion of the effects of arbitrary tunnel couplings.

[42] D. Zwillinger, V. Moll, I. Gradshteyn, and I. Ryzhik, *Table of Integrals, Series, and Products*, 8th ed. (Academic, Cambridge, 2014)

[43] T. V. Shahbazyan and M. E. Raikh, Two-channel resonant tunneling, Phys. Rev. B **49**, 17123 (1994).

[44] B. Kubala and J. König, Flux-dependent level attraction in double-dot Aharonov-Bohm interferometers, Phys. Rev. B **65**, 245301 (2002).

[45] J. Rammer, *Quantum Field Theory of Non-equilibrium States* (Cambridge University Press, Cambridge, 2007)

[46] A. Mitra, I. Aleiner, and A. J. Millis, Phonon effects in molecular transistors: Quantal and classical treatment, Phys. Rev. B **69**, 245302 (2004).

[47] P. Stadler, W. Belzig, and G. Rastelli, Ground-State Cooling of a Carbon Nanomechanical Resonator by Spin-Polarized Current, Phys. Rev. Lett. **113**, 047201 (2014).